A Vector-Based Flexible-Complexity Tool for Simulation and Small-Signal Analysis of Hybrid AC/DC Power Systems

Andrés Tomás-Martín[a], Carlos David Zuluaga-Ríos[a], Jorge Suárez-Porras[a], Behzad Kazemtabrizi[b], Javier García-Aguilar[a], Lukas Sigrist[a], Aurelio García-Cerrada[a]

[a]*Institute for Research in Technology, Comillas Pontifical University, Alberto Aguilera, 23, 28015, Madrid, Spain*
[b]*Engineering Department, Durham University, Durham, United Kingdom*

Abstract

This paper presents VFlexP, an open-source, vector-based tool for the time domain simulation, static analysis, and small-signal analysis of hybrid AC/DC power systems, built upon MATLAB-Simulink. Unlike existing tools such as PowerFactory, Simplus Grid Tool, and PSCAD, VFlexP allows for a flexible-complexity representation of all devices without taking any traditional simplification for granted, and the seamless inclusion of new models without extensive modifications. VFlexP has a module to analyse the relevance of the state variables of the model in a given input-output relationship. This information can then be used to simplify the model in subsequent studies. VFlexP has been designed to obtain an accurate initial point for simulation from a conventional power-flow analysis in order to achieve fast initialisation without troublesome and time-consuming initial transients. The tool's graphical user interface groups all power system elements of the same type in a single block, even if they have different parameters, providing a clean representation even for large systems. These characteristics make VFlexP a valuable tool for the detailed analysis and non-linear time simulation of hybrid power systems in a fast-changing scenario, even though, for the time being, the analysis and simulation carried out are limited to a d-q representation of a balanced power system.

Keywords: Flexible complexity, model reduction, small signal analysis, vector-based

1. Introduction

As many countries transition towards low-carbon or net zero-carbon energy systems, renewable energy sources (RESs) are playing an increasingly important role in the energy mix, transforming the way power systems are operated. RESs present unique new challenges: they are often not readily dispatchable; require inverter-based interfaces with the grid (i.e, inverter-base resources or IBRs); and are typically distributed across the grid as distributed energy resources (DERs) [1]. In response to these challenges, hybrid AC/DC systems have become increasingly important for integrating diverse energy sources into the grid, thanks to the advances in DC/AC electronic power converters. The combination of AC and DC technologies should improve grid flexibility, stability, and resilience, facilitating a smoother transition to renewable-dominated power systems and supporting long-term sustainability and low-carbon goals.

Conventional tools for the analysis of AC electric power systems address one or more of the following aspects [2]:

- Static analysis, mainly power flow (PF) and optimal power flow (OPF), that determines the system voltages, currents, and power flows under stable steady-state operating conditions.
- Dynamic analysis consisting of time-domain (TD) simulation and/or small-signal analysis (SSA).

There are two distinctive approaches among time-domain simulators. On the one hand, Transient Stability (TS) Simulators, also called Electromechanical (EM) Simulators, study the effects of disturbances on synchronous generator dynamics. They neglect the dynamics of the electrical grid (which is assumed to be in a quasi-steady state) because they are very fast and generally well-damped and focused on the dynamics of electromechanical components with often lightly-damped low-frequency oscillations. These simulators provide phasor information for voltages and currents and this is why they are often called RMS simulators. On the other hand, Electromagnetic Transient (EMT) simulators use detailed models of all components [3, 4] to study fast transients where phasor modelling is not appropriate and can be computationally intensive [5].

Finally, SSA is a method for evaluating system stability and dynamic response to small disturbances by linearising the system around an operating point, allowing engineers to assess how minor changes impact stability and interactions across components or design control strategies and improve system resilience [6].

Email address: atomas@comillas.edu (Andrés Tomás-Martín)

Gradually, most analysis tools have incorporated, in one way or another, hybrid AC/DC systems. For example, static analysis can be carried out with MATPOWER [7] and its extension FUBM [8], MatACDC [9], and PyACDC [10]. In addition, EMT and/or EM simulation is possible with PowerFactory [11], PSCAD [12], ETAP [13] and PSS/E [14]. SSA can be carried out with PowerFactory, CSTEP [15] and DSATools [16]. The capabilities of several of these important tools have been summarized in Table 1 indicating whether they are commercial $\mathbb{P}$, open-source $\mathbb{O}$, or toolboxes of MATLAB-Simulink which is a commercial software package $\mathbb{OM}$.

Nowadays, IBRs (or, in other words, fast-acting electronics-base generators) are becoming increasingly present in electric power systems, and the question of whether the time-scale separation between generators and grid can be taken for granted may not always have a unique answer [27]. However, none of the above-mentioned software tools addresses this question directly. This new scenario underscores the need for more flexible and multi-purpose tools.

This paper presents VFlexP, an open-source tool for hybrid AC/DC power system analysis and simulation built upon MATLAB/Simulink. Component data are fed into the system description with a file similar to the one used in MATPOWER, and the electrical system is described using a synchronously rotating d-q reference frame with Simulink dynamic blocks. Only elementary blocks such as integrators, sums, products, gains, and trigonometric functions are used for device-model building to ease linear analysis. Static analysis of the electrical system, such as PF and OPF, can be performed using a modified version of MATPOWER, as outlined in [8], enabling support for hybrid AC/DC systems. Additionally, the proposed tool supports SSA for hybrid systems with a high penetration of IBRs, facilitating deep system insights. As part of this analysis, it also quantifies the state relevance (SR) in the input-output response of dynamic hybrid AC/DC systems and the result can later be used for an informed model reduction. VFlexP accommodates flexible modelling with options for varying levels of detail in the component models. EMT simulation is carried out by default, but the use of simplified component models makes less cumbersome simulation possible. Simulations can be conducted using either the original non-linear model or a linearised approximation, with the flexibility of selecting from a full-order model or several reduced-order approximations.

If compared to other tools included in the literature survey, the following features can be highlighted:

- The static analysis can deal with AC and DC systems seamlessly. Several devices are already available in the library. Some of them are to be connected to the DC side.
- Grid-forming or grid-following control of IBRs and AC/DC interface converters can be represented and used.
- Special care has been taken to derive an accurate calculation of the operating point of the full system starting from the PF results of MATPOWER. This avoids unrealistic and time-consuming transients when starting a simulation and makes it possible for seamless system linearisation.
- Primary and secondary frequency and voltage control layers for generators are included, with flexible architecture choices.
- Most blocks used in the Simulink workspace already have linearised versions in Simulink original library, and MATLAB uses them for reliable linearisation. Those not in the library have been linearised using a Taylor expansion and stored for subsequent use. This avoids calculating the linear approximation by finite differences.

The following contributions of the tool can be highlighted:

- In addition to a full-featured SSA of the system (i.e. calculation of participations, eigenvalue sensitivity, mode shapes, etc.), the user can analyse the relevance of all state variables in the input-output response of the non-linear system. This is an excellent starting point towards the order reduction of the original model.
- Only one block is necessary in Simulink workspace to represent all devices of the same type, and the same level of detail, even if they have different parameters. This is possible thanks to the vectorisation of all the differential equations used, which largely reduces computational effort.
- Each device block can host several levels of detail for a given component. The level to be used, according to a previous relevance analysis, can be easily selected by using a GUI, which implements the concept of flexible complexity and allows improving computation efficiency further.

The rest of the paper is organized as follows: Section 2 details the vector-based and flexible-complexity approach of hybrid power systems used in VFlexP. Section 3 describes how the SSA and simulations are carried out after initialising the system around an operating point. In Section 4, SSA and simulation results are shown by comparing VFlexP with another simulation tool and considering different grid sizes. Moreover, a reduced-order model of a large power system is validated. Finally, Section 5 concludes the paper.

2. Vector-based modelling of hybrid power systems with flexible complexity

2.1. Scalable and Vectorisable Modelling of power systems

The simplest components included in VFlexP's library are inductors (L-R series connected) and capacitors (C-R

Table 1: Overview of simulation and analysis tools for hybrid AC/DC power systems. In License: $\mathbb{O}$ means open-source, $\mathbb{P}$ means commercial, and $\mathbb{OM}$ means open-source tools that rely on MATLAB and/or Simulink.

Tool	PF	OPF	SSA	SR	License	EMT	RMS
DSATools [16]	✓		✓		$\mathbb{P}$		
ETAP [13]	✓	✓			$\mathbb{P}$	✓	✓
Neplan [17]	✓	✓	✓		$\mathbb{P}$	✓	✓
PowerFactory [11]	✓	✓	✓		$\mathbb{P}$	✓	✓
PSCAD [18]	✓				$\mathbb{P}$	✓	
PSS/E [14]	✓	✓	✓		$\mathbb{P}$		✓
Smart Flow [19]	✓	✓	✓		$\mathbb{P}$		✓
ANDES [20]	✓		✓		$\mathbb{O}$	✓	
DPsim [21]	✓				$\mathbb{O}$	✓	✓
PowerSimulationsDynamics.jl [22]	✓		✓		$\mathbb{O}$	✓	
Pypower and PyACDC [10]	✓	✓			$\mathbb{O}$		
CSTEP [15]			✓		$\mathbb{OM}$	✓	✓
MATPower and MATACDC [7, 9]	✓	✓			$\mathbb{OM}$		
MATLAB/Simulink and MatDyn [23]					$\mathbb{OM}$	✓	✓
PSAT [24]	✓		✓		$\mathbb{OM}$		✓
SimplusGT [25]	✓		✓		$\mathbb{OM}$	✓	
SSMD [26]			✓		$\mathbb{OM}$		
VFlexP	✓	✓	✓	✓	$\mathbb{OM}$	✓	✓

parallel connected). The differential equations governing the behaviour of a series RL in a synchronous d-q frame are typically written as follows in per unit (pu):

$$v_d = \frac{1}{\omega_{base}} L \frac{di_d}{dt} - \omega L i_q + R i_d, \tag{1}$$

$$v_q = \frac{1}{\omega_{base}} L \frac{di_q}{dt} + \omega L i_d + R i_q, \tag{2}$$

where, v_d and v_q are the d- and q-axis voltages, respectively, across the RL element, i_d and i_q are the d- and q-axis currents, respectively, ω_{base} is the base frequency of the system (in rad/s), ω is the angular speed of the synchronously rotating frame, and R and L are the resistance and inductance values of the series RL element, respectively. If v_d and v_q (inputs) are known, differential equations (1) and (2) can be integrated to calculate i_d and i_q (outputs and state variables). These differential equations can be easily built using elementary Simulink blocks (integrators, sums, and gains with the parameters), and they can be included in a user-defined block. However, a power system is bound to have a large number of RL elements as part of power lines and/or loads, for example, and including a block for each line in Simulink's workspace is not practical. Instead, a single block can be used to contain all the elements of the system with equations like (1) and (2), if those equations are vectorised as follows:

$$\mathbf{v_d} = \frac{1}{\omega_{base}} \mathbf{L} \odot \frac{d\mathbf{i_d}}{dt} - \omega \mathbf{L} \odot \mathbf{i_q} + \mathbf{R} \odot \mathbf{i_d}, \tag{3}$$

$$\mathbf{v_q} = \frac{1}{\omega_{base}} \mathbf{L} \odot \frac{d\mathbf{i_q}}{dt} + \omega \mathbf{L} \odot \mathbf{i_d} + \mathbf{R} \odot \mathbf{i_q}, \tag{4}$$

where voltages, currents and each type of parameter are grouped in vectors (i.e., $\mathbf{v_d}$, $\mathbf{v_d}$, $\mathbf{i_d}$, $\mathbf{i_q}$, $\mathbf{L}$, and $\mathbf{R}$); and multiplications and sums are carried out element-by-element (i.e., Hadamard product $\odot$).

Similarly, all elements included so far in VFlexP (capacitors, loads, synchronous generators, electronic power converters, etc.) can be represented in vector form. Therefore, only one block needs to be included in Simulink's workspace to contain all elements of the same type and model.

2.2. Flexible-complexity models for power systems

In traditional power systems, the slow electromechanical dynamics of synchronous generators could be decoupled from the fast response of inductors and capacitors that power lines consist of [27]. Nowadays, this separation is challenged by the fast response of electronic-based generation or IBRs, and it cannot be taken for granted that all fast dynamics (e.g., inductors) can always be simplified. The same type of element may require a different level of detail depending on its position in the power grid or even on the operating point where the study is being carried out. Bearing this in mind, VFlexP has been designed so

that each element can be included with a different level of detail. For example, if the dynamics of a number of inductors can be neglected (i.e., $di_{dq}/dt = 0$), equations (3) and (4) can easily be simplified into vectorise algebraic equations where currents can be calculated if voltages are known. Each block of the library in VFlexP offers multiple suggested levels of detail, allowing easy selection of the appropriate level. However, within the Simulink workspace, each block can only contain elements of the same type represented at an identical level of detail. For instance, if M inductors require the description in (1) and (2), while D inductors can be represented with $di_{dq}/dt = 0$, two separate blocks will be needed in the Simulink workspace: one for M inductors and another for D inductors. Selector and assignment blocks have been used for each component model to select its level of detail, as shown in Fig. 1 for a typical load. In this figure, the load models are organized into two levels of detail (e.g., A and B) to represent different modelling complexities. The voltage ($\mathbf{v}$) and current ($\mathbf{i}$) vectors are structured with three rows, representing the direct (d), quadrature (q), and homopolar components (with the homopolar component neglected in this example). Each load type, such as A and B, is connected to different groups of buses, where N denotes the total number of buses in the system, and N_A and N_B represent the number of buses with load types A and B, respectively. For each load type, voltage and current vectors are labelled according to load type and bus assignment. For instance, the notation $\mathbf{v}_A^{[3\times N_A]}$ and $\mathbf{i}_A^{[3\times N_A]}$ designates the dimensions of the voltage and current array corresponding to type A loads across N_A buses. This notation specifies a clear vector structure that accommodates varying load models across buses. The current vector through each load is calculated from its parameters and voltage vector, depending on the load model. To consolidate the currents of all load types into a single current array $\mathbf{i}^{[3\times N]}$, an assignment block is employed. This block assigns each load type's current at a given bus k to the corresponding position in $\mathbf{i}^{[3\times N]}$. If no load of type A is connected at bus k, the 3 rows of the k-th column of the current array are set to zero; otherwise, it contains the current value for the load connected at that bus. This approach to array assignment applies similarly to other elements in VFlexP, such as generators, transmission lines, and both AC and DC loads. A comprehensive list of the models included in VFlexP, detailing components like generators and converters, is provided in Figure 2 and Table 2, highlighting the modularity and flexibility of VFlexP's modelling framework.

3. Simulation of hybrid power systems and SSA in VFlexP

This section describes VFlexP capabilities to simulate and analyse hybrid power systems. VFlexP runs a power flow to initialise the state variables accurately, which is

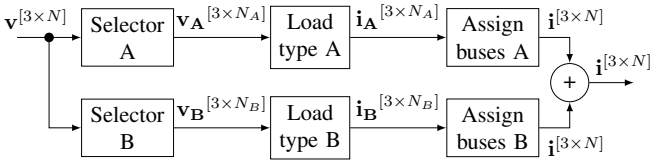

Figure 1: Loads, selectors and assignments. Array dimensions are indicated in square brackets. All arrays have 3 rows, direct (d), quadrature (q) and homopolar (neglected for the time being) components. N is the number of buses in the system, N_A, N_B and N_C are the number of Loads of type A, B and C in the system, respectively.

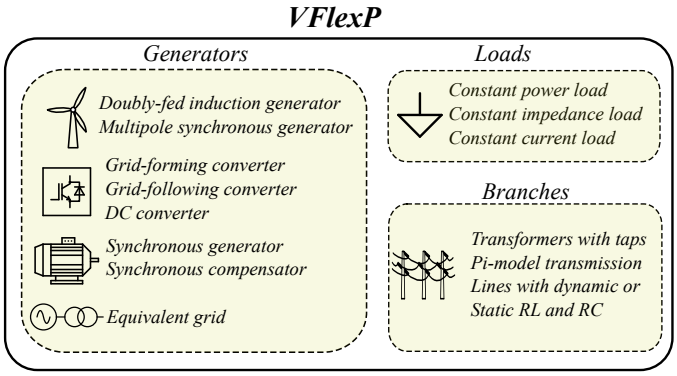

Figure 2: Summary of elements included in VFlexP.

needed for non-linear time-domain simulations and SSA. With respect to SSA, VFlexP derives a linear approximation of the non-linear system included in the Simulink workspace, and it can carry out a comprehensive eigenvalue analysis of the resulting linear system. The tasks corresponding to these capacities are addressed in the following sections.

3.1. Powerflow and Initialisation

Before linearising a Simulink model, the target steady-state operation point must be calculated, i.e., the initial values of all the state variables of the system must be determined. This can be done directly with the original tools in MATLAB/Simulink (e.g., *findop*), but they are not very efficient when dealing with large dynamic systems. Alternatively, VFlexP uses the following strategy:

1. Grid currents and voltages are initialised by running a power-flow algorithm based on MATPOWER [7], which is a well-known open-source MATLAB tool originally developed to be applied on AC power systems, only. This tool has been extended with the flexible universal branch model (FUBM) [8] to seamlessly deal with hybrid AC/DC power systems. The power flow solution includes the values for voltage amplitude and angle, and active and reactive power injections of all generators at their bus of connection. However, it does not include the value of internal state variables, for example those associated with current or voltage controllers in electronic generators.

Table 2: Summary of elements included in VFlexP.

Element	Implemented model
Synchronous Generators	Eighth-Order model with Governor and AVR [6] Second-Order model [25] Multi-pole model [28]
Induction Generators	Conventional model [6]
Synchronous Compensators	Conventional model [6]
Doubly Fed Induction Generators	Conventional model [29]
AC Loads	Static Loads [6] Dynamic Loads [6] Induction Motors [6]
AC Transformers	Conventional model [6]
DC loads	Static Loads [6] Dynamic Loads [30]
Converters	Grid-forming converter (droop) [31] GFr (Virtual Synchronous Machine) [32] Grid-following converters [31] Grid-following interface converters [31] Buck DC-DC converters [25]

2. State variables not calculated by the initial PF run can be calculated automatically using a gradient-based optimisation in MATLAB for each one of the blocks in the Simulink workspace. The results of the PF run are the restrictions to be satisfied by the optimisation process. In addition, for simple blocks, the equations to calculate the initial conditions can be calculated manually in advance and stored in the block for future use. The impedance value of constant-impedance loads is recalculated in this process to ensure that they consume the active and reactive power given by the PF solution.

3.2. Linearisation

For linearisation, VFlexP uses MATLAB function `linearize(mdl, io, op)`, where `mdl` is the name of the Simulink model, `io` is the set of inputs and outputs to consider in the linear model (previously set using `setlinio` function), and `op` is the operation point used for the linearisation. Considering that operating point, MATLAB calculates the input and state values for each block and requests its Jacobian. The models included in VFlexP mainly include Simulink basic blocks (*e.g.,* integrators, products, sums, switches, etc.). These blocks have a predefined Jacobian for linearisation. For other more complex blocks used, the Jacobian in the operating point is provided. With the Jacobian for all blocks, Simulink considers how the blocks are connected with each other to compute the complete linear model of the system. The final linear system obtained using this method is of the form:

$$\begin{cases} \dot{x} = \mathbf{A}x + \mathbf{B}u \\ y = \mathbf{C}x + \mathbf{D}u \end{cases} \tag{5}$$

where x is the system state column vector, u is the input vector, y is the output vector, and $\mathbf{A}$, $\mathbf{B}$, $\mathbf{C}$ and $\mathbf{D}$ are the system matrices.

3.3. Small signal analysis

The mode-in-state participation factors normalised as in [2] and [33] (based on [34]) are used here:

$$p_{ji} = \frac{|w_{ij}|\,|v_{ji}|}{\sum_{\forall k}|w_{ik}|\,|v_{ki}|} \tag{6}$$

where p_{ji} is the normalised mode(i)-in-state(j) participation factor in a linear system, v_{ji} is the element of the $j-th$ row and $i-th$ column of matrix $\mathbf{V}$ of right column eigenvectors of $\mathbf{A}$ and w_{ij} is the element of the $i-th$ row and $j-th$ column of matrix $\mathbf{W}$ of left row eigenvectors of $\mathbf{A}$ calculated as $\mathbf{W} = \mathbf{V}^{-1}$.

The state relevance presented in [35], included in this tool, measures the importance of the dynamics of each state in the input-output response of the system. This algorithm uses the balanced transformation of the linearised system, presented in [36] and implemented using `balanced_system = balreal(linear_system)` command in MATLAB. The state relevance is calculated as:

$$\hat{\mathbf{R}}_x = \mathbf{P} \cdot \left([g_1, \cdots, g_n] \cdot \bar{\mathbf{P}}\right)^T \tag{7}$$

where g_i is the Hankel singular value of state i, $\mathbf{P}$ is the participation matrix of the original system and $\bar{\mathbf{P}}$ is the participation matrix of the balanced system. The state relevance can be normalised as:

$$\mathbf{R}_x = [R_x(x_1), \ldots, R_x(x_n)]^T = \hat{\mathbf{R}}_x / \sum_{\forall i}\left(\hat{R}_x(x_i)\right) \tag{8}$$

The sensitivity of an eigenvalue of A to changes in a parameter α, introduced by [37], can be calculated as by [38]:

$$\frac{\partial \lambda_i}{\partial \alpha} = \frac{\mathbf{w}_i^{\mathrm{T}} \cdot \dfrac{\partial \mathbf{A}}{\partial \alpha} \cdot \mathbf{v}_i}{\mathbf{w}_i^{\mathrm{T}} \cdot \mathbf{v}_i} = \mathbf{w}_i^{\mathrm{T}} \cdot \frac{\partial \mathbf{A}}{\partial \alpha} \cdot \mathbf{v}_i \tag{9}$$

where λ_i is the ith eigenvalue of the system and $\mathbf{v}$ and $\mathbf{w}_i^T$ are the right and left eigenvectors associated to λ_i, respectively. VFlexP calculates $\partial\mathbf{A}/\partial\alpha$ by finite differences.

The tool also includes mode-shape calculation. For a given eigenvalue λ_i of matrix $\mathbf{A}$ in (5), the mode shapes are the complex numbers that form the right eigenvector corresponding to that eigenvalue (one complex number per state variable). Mode shapes illustrate the relative phase of mode oscillations which has application in power system stabiliser design and inter- and intra-area oscillation analysis.

3.4. Simulation of non-linear and linear models

VFlexP models each element of hybrid power systems using basic Simulink blocks such as sums, products, and

integrators to define the differential equations. As a result, it leverages all the capabilities of native Simulink. For example, variable-step solvers can be used. They are particularly useful when the steady state is reached since the variables of a balanced three-phase power system remain constant in the d-q reference frame. Additionally, Simulink solvers for stiff differential equations can significantly speed up simulations, especially given the different time scales often involved in the system's dynamics. Another important feature is that Simulink supports real-time simulation on most RT boxes available on the market, including OPAL-RT [39].

Linearised models are simulated using `lsim( linearised_system,u,t)` command of MATLAB, where `u` is the input to the system and `t` is the time vector for the simulation. Command `lsim` discretises the linear system with `c2d` function, using, by default, a zero-order hold and then calculates the response to the input.

4. Case studies using VFlexP

This section demonstrates the main features of VFlexP through case studies on small and large hybrid AC/DC power systems. The performance is compared with the Simplus Grid Tool [25], a recently presented open-source tool also based on MATLAB-Simulink. Four test systems are analysed, focusing on voltage and frequency responses, power delivery, and eigenvalue analysis. VFlexP's ability to handle non-linearities and SSA is demonstrated. The usefulness of the concept of state relevance for model-order reduction without compromising accuracy is also discussed.

4.1. Case study: small power systems

This section explores the application of VFlexP in three small power systems (see Figures. 3, 5 and 7).

All the parameters for the systems shown in Figures 3 and 7 can be found in the examples in SimplusGT repository [25] but have also been included in Appendix A. For comparison, a 50-second dynamic simulation was carried in all three small systems starting from an operating point determined by the load values shown in Figures 3, 5 and 7. The load in the three systems was increased between 25 and 26.2 seconds. Simulation results for the two simulation tools applied to the three systems were recorded, and voltage, speed, active, and reactive power of the synchronous machine are shown in Figs. 4, 6 and 8. The blue line is the response obtained using SimplusGT, and the red dotted line is the one obtained with VFlexP.

The first test system (Fig. 3) includes a synchronous generator connected to a load. Fig. 4 shows the simulation results of this system. Simplus calculates the voltage behaviour of a synchronous machine with adequate accuracy in the dynamic simulation. However, the tool lacks

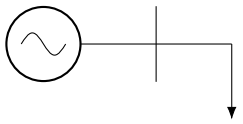

Figure 3: Single-line diagram of a synchronous generator feeding a load

Table 3: Eigenvalues for the system shown in Fig. 3.

	Simplus		**VFlexP**	
	$\mathrm{Re}\,(\lambda)$	$\mathrm{Im}\,(\lambda)$	$\mathrm{Re}\,(\lambda)$	$\mathrm{Im}\,(\lambda)$
1	0.0000	0.0000	–	–
2	$-2.8e-09$	0.0000	–	–
3	**−0.0341**	**0.0000**	**−0.0340**	**0.0000**
4	**−0.0495**	**−50.00**	**−0.0487**	**−49.99**
5	**−0.0495**	**50.00**	**−0.0487**	**−49.99**
6	**−2019.9**	**−50.00**	**−2020.2**	**−50.00**
7	**−2019.9**	**50.00**	**−2020.2**	**50.00**
8	–	–	$-1e15$	0.0000
9	––	–	$-1e15$	0.0000
10	–	–	$-1.2e07$	−49.96
11	–	–	$-1.2e07$	49.96

an accurate procedure to compute the initial operating point of the dynamic simulation and an unnecessary initial transient takes place. The voltage response on the machine using Simplus remains close to 1 pu during the simulation, which reflects good control and stability of the system. VFlexP accurately calculates the initial operating point and produces dynamic simulation results very close to those produced by Simplus without the initial unnecessary transient. The transient response, when the load changes, is very similar in the two simulation tools, even in those variables that show important oscillations (Notice the close response of the two tools in the zoomed windows in Figs 4-(c) and (d)). Fig. 4 shows the location of five eigenvalues of the linear approximation of the system shown in Fig. 3. Simplus and VFlexP produce very similar results. However, both tools must add extra elements to include all the state variables of interest. For example, VFlexP adds a small shunt capacitor (i.e., 1×10^{-6} pu) at each of the buses so that bus voltages become state variables and, in this case, it adds a transmission line with a very small resistance (0.1×10^{-6} pu) between the generator and the load. These additional state variables produce additional eigenvalues in the linear approximation of the original system (see Table 3 for a comparison of the eigenvalues calculated by the two tools). The additional eigenvalues produced by VFlexP can be spotted very easily due to their unreasonably large moduli. However, the extra eigenvalues produced by Simplus are unstable or very close to become unstable. Finally, Fig. 4-(f) shows the response of the system frequency for the non-linear simulation and its linear approximation using the proposed tool. The two curves agree closely.

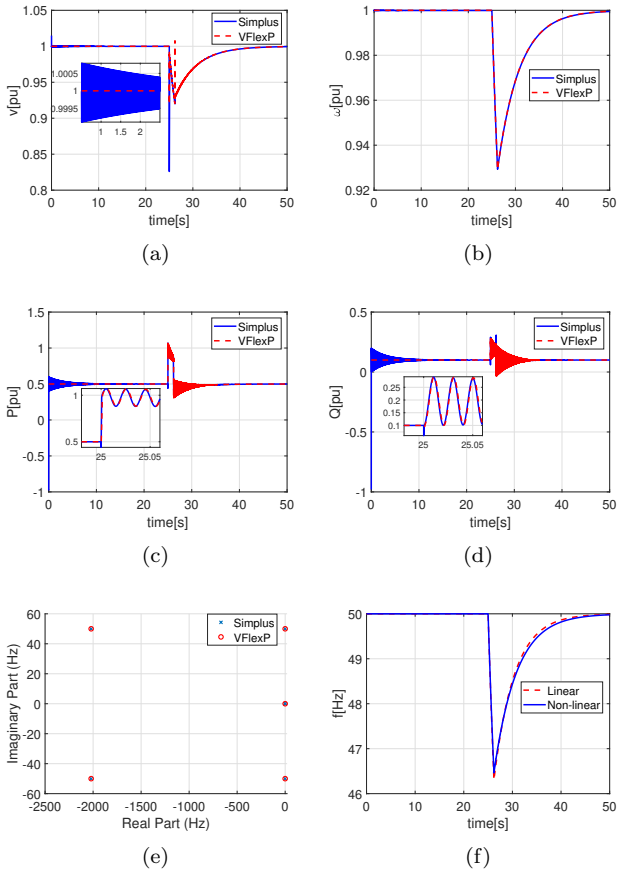

Figure 4: (a) Bus-1 voltage, (b) Speed of the SG in pu, (c) Active power of the SG, (d) Reactive power of the SG, (e) eigenvalues of the system and (f) Comparison of the frequency response of non-linear and linearised system shown in Fig. 3.

In the second system (Fig. 5), data from the first system were reused, and a purely inductive transmission line with a reactance of 0.65 pu ($X_{12} = 0.65$ pu) was added. Simplus and VFlexP were compared in this set-up. Again, a load change was introduced from 25 to 26.2 seconds, and the results are shown in Fig. 6. Fig. 6-(a), 6-(c), and 6-(d) highlight initialization issues associated with Simplus. Meanwhile, Fig. 6 (e) presents some of the eigenvalues for the system in Fig. 5. In this case, some of the eigenvalues calculated with Simplus have positive real parts (Table 4). This table also shows that Simplus employs 15 state variables, whereas the proposed tool only uses 11. An analysis of the simulation results in Figures 6-(e) and 6-(f) demonstrates that the proposed tool accurately models the system, confirming its local stability around the operating point. Figs. 6-(e) and 6-(f) shows that linearisation provides a good approximation of the nonlinear system in the vicinity of the operating point.

Finally, the 4-bus hybrid AC/DC power system presented by Zheng et al. in [40] was also studied (see Fig. 7). A synchronous generator is connected to bus 1 (AC side), a buck converter is connected to bus 4 (DC side), and

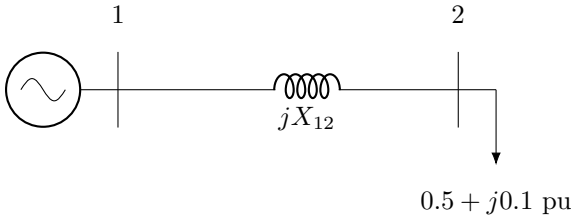

Figure 5: Single-line diagram of a synchronous generator feeding a load through a transmission line.

Table 4: Eigenvalues for the system shown in Fig. 5.

	Simplus		**VFlexP**	
	Re (λ)	Im (λ)	Re (λ)	Im (λ)
1	0.0000	0.0000	–	–
2	$-2.0e-15$	-50.00	–	–
3	$-2.0e-15$	50.00	–	–
4	$2.9e-14$	-50.00	–	–
5	$2.9e-14$	50.00	$-3.5e07$	-50.00
6	$-5.3e-14$	-50.00	$-3.5e07$	50.00
7	$-5.3e-14$	50.00	$-3.3e01$	$-2.3e05$
8	$-9.8e-16$	0.0000	$-3.3e01$	$2.3e05$
9	$4.4e-06$	0.0000	$-3.3e01$	$-2.3e05$
10	$-4.9e-06$	0.0000	$-3.3e01$	$2.3e05$
11	**-0.0304**	**0.0000**	**-0.0304**	**0.0000**
12	**-0.0632**	**-50.00**	**-0.0632**	**-50.00**
13	**-0.0632**	**50.00**	**-0.0632**	**50.00**
14	**$-1.1e02$**	**-50.00**	**$-1.1e02$**	**-50.00**
15	**$-1.1e02$**	**50.00**	**$-1.1e02$**	**50.00**

AC and DC sides are connected by a grid-following interface converter placed between buses 2 and 3 with a traditional droop control structure and PI voltage and current controllers in cascade, with a LCL output filter. The generator and the two electronic converters in Fig. 7 feed three active power loads. Fig. 8 shows the behaviour of this system when using Simplus and VFlexP. Due to the aforementioned comments regarding the number of eigenvalues, only the time responses to load variations at bus 2 were compared. Figures from 8-(a) to 8-(d) demonstrate the close agreement between the simulation results using Simplus and those using VFlexP. In addition, Fig. 8-(e) shows that the simulations of the non-linear system and its linear approximation carried out using VFlexP agree closely.

The computation times (CT) required for both tools to perform the dynamic simulations presented in Figs. 4, 6 and 8 are written in Table 5. To ensure a fair comparison with VFlexP, Simplus was adjusted to use a variable integration step instead of its default fixed discrete time step. All simulations were performed on an Intel Core i7 PC with a 2.8 GHz processor. VFlexP consistently outperforms Simplus across all three systems in terms of computation time. The difference is most pronounced in the Hybrid System, where VFlexP requires only 11.687 seconds, compared to 103.84 seconds required by Simplus (i.e., a reduction of about 89%). Both tools take longer to simulate

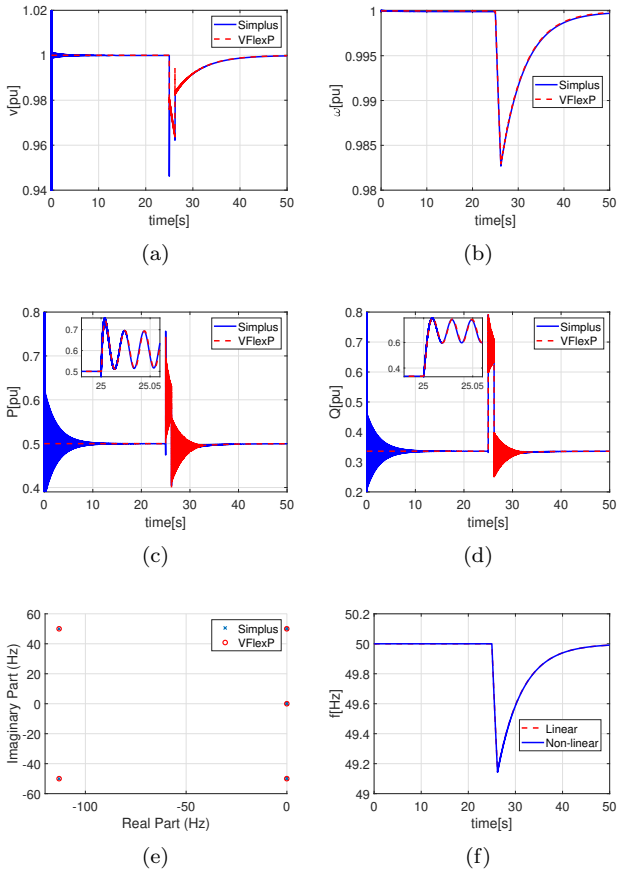

Figure 6: (a) Bus-1 voltage, (b) Speed of the SG in pu, (c) Active power of the SG, (d) Reactive power of the SG, (e) eigenvalues of the system and (f) Comparison of the system (Fig. 5) frequency with non-linear and linearised models.

Table 5: Computation time when Simplus and VFlexP tools to simulate the systems shown in Figs. 3, 5 and 7.

Tool	Computation time $[s]$		
	SG	**Two Bus System**	**Hybrid System**
Simplus	33.625	36.843	103.84
VFlexP	12.312	15.953	11.687

the hybrid system due to its intricate dynamics involving both AC and DC elements.

4.2. Case study: Large hybrid AC/DC power system

4.2.1. Exploring reduced order models for a large hybrid power system

To validate the performance of the proposed tool on large hybrid AC/DC power systems, the hybrid power system introduced in [41] was implemented in the tool. Figure 9 shows the schematic diagram of that power system, automatically generated by the tool, consisting of two AC areas connected through two DC grids by means of several DC/AC converters. VFlexP includes in this graph the active and reactive power generated by units and consumed by loads at every bus, resulted by the power flow calculation.

AC area 1 is the IEEE 57-bus system, and AC area 2 is the IEEE 14-bus system. Buses with generators are highlighted in red. All the static data of the test case were taken from [41]. The model and parameters for the generator included in bus 9 of the DC grid are the ones used for the DC generator in [40]. All the generators on the AC grids are modelled as grid-forming converters with the a traditional droop control structure and PI voltage and current controllers in cascade, with a LCL output filter. The details of the control structure of the converters can be found in [31]. To illustrate the advantages of the vectorisation used in the presented tool, Figure 10 shows one screenshot of the Simulink workspace containing the hybrid system implemented in VFlexP. The blocks used to implement the large hybrid system shown in Figure 9 are the same as the ones used to implement the small hybrid system used in Figure 7 (with the only difference that the synchronous generator block was replaced by the grid-forming block). Notice that, in the system of Figure 9, the resulting vectors are larger because the system implemented is larger, but the number of Simulink blocks does not change.

The system was linearised in the operating point calculated by the initialisation of all variables from the results of the power-flow analysis given by [8] with the set-points of [41]. Then, the state relevance of each state of the linear system in the system input-output response is calculated as described in [35] and grouped by type of element as shown in Figure 11. The inputs chosen for the linear model are current injections on each AC bus, and the outputs are the frequencies of all grid-forming converters.

As shown in Figure 11, the dynamics of all DC elements, load dynamics and some dynamics of the grid-forming converters (GFrs) have very little contribution to the input-output response of the linear system. However, some dynamics of the GFrs, branches and buses can not be neglected because they have a considerable contribution to the input-output response (*i.e.,* not negligible state relevance).

To show the usefulness of the state relevance measure, the following scenario is proposed: the system in this large case study is modified by changing the voltage controller of DG1.

Figure 12 shows the evolution of the state relevance of the voltage and current controllers for all converters of the system under study when varying the voltage controller of converter DG1: the integrator gain of the voltage controller of DG1 was increased from its initial value (the value of the integrator gain of the voltage controller of all other DGs) to 10 times its initial value.

As Figure 12 clearly shows, the state relevance of the states of the voltage and current controllers of DG1 increase with the integrator gain of the voltage controller of DG1. This result can be understood by considering that the varying control system is approaching instability. However, the state relevance of the states of the voltage and current controllers of DG2 also increase with the in-

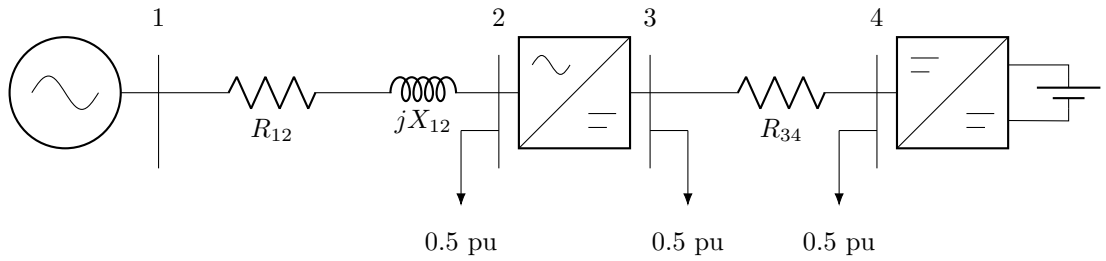

Figure 7: Single-line diagram of 4-bus hybrid AC-DC system presented by [40]

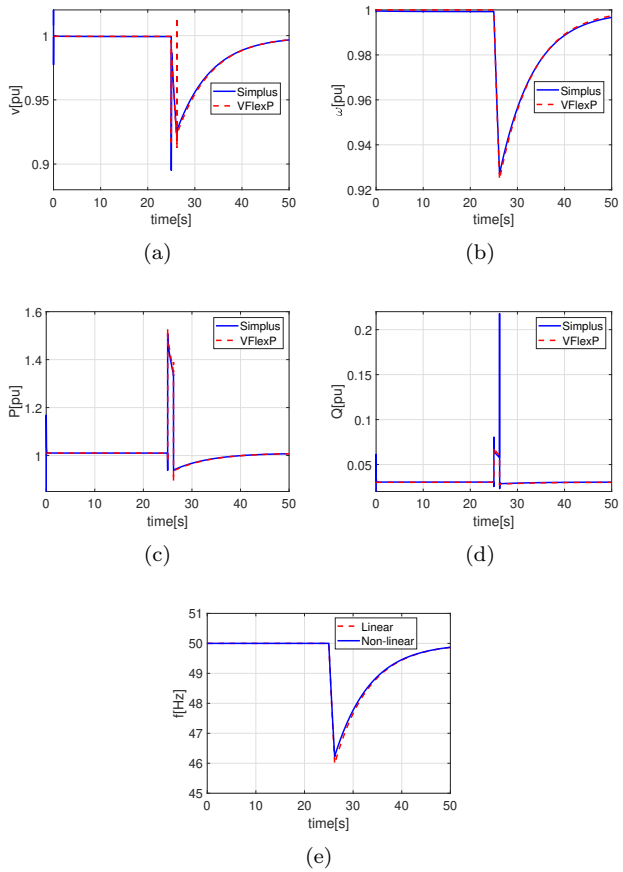

Figure 8: (a) Bus-1 voltage, (b) Speed of the synchronous generator in pu, (c) Active power, (d) Reactive power and (e) Frequency in the non-linear and linearised simulations of the system in Fig. 7.

tegrator gain of the voltage controller of DG1. This is due to the fact that DG2 is close to DG1 in terms of electrical distance.

To further validate the state relevance analysis, the response of the complete non-linear system to a load change is compared with the response of several non-linear systems with different levels of complexity reduction:

- VCC 1-12: Complete model.
- VCC 1-2: The dynamics of AC branches, loads and grid-forming converter voltage and current controls with state relevance below 0.0012 are neglected.

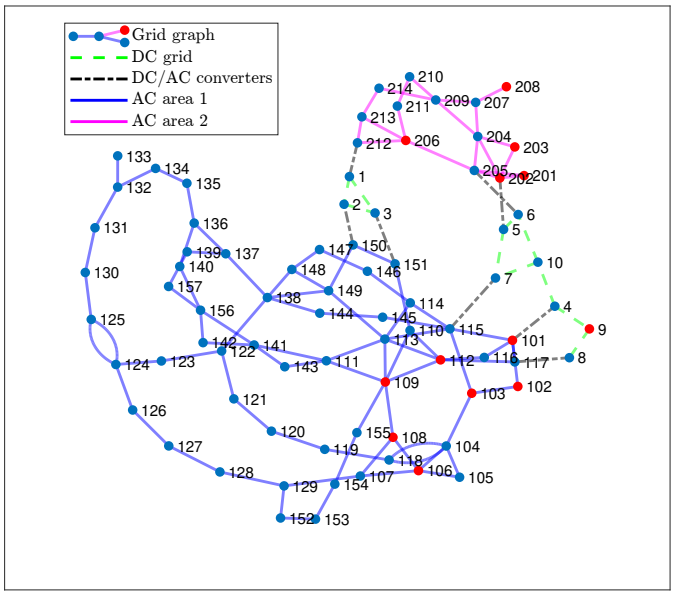

Figure 9: Graph representing the grid used for the case study. Buses highlighted in red include generation.

- VCC 1: The dynamics of AC branches, loads and grid-forming converter voltage and current controls with state relevance below 0.004 are neglected.
- No VCC: The dynamics of AC branches, loads and grid-forming converter voltage and current controls are neglected.

Figure 13 shows the comparison of the complete and reduced models to a load increment in bus 10. The variable compared is the frequency of DG1 (grid-forming converter at bus 101).

As clearly shown in Fig. 13, the frequency of DG1 has a lightly damped oscillation when the load change is applied. This oscillation is only properly captured when the dynamics of the states with relatively high relevance are not neglected. In any reduced-order model, the dynamics of the states with higher state relevance must be conserved.

4.2.2. An example of the use of the "state relevance" calculated by VFlexP

The connection of a grid-following converter at bus 101 has been explored with the use of the concept of "state rel-

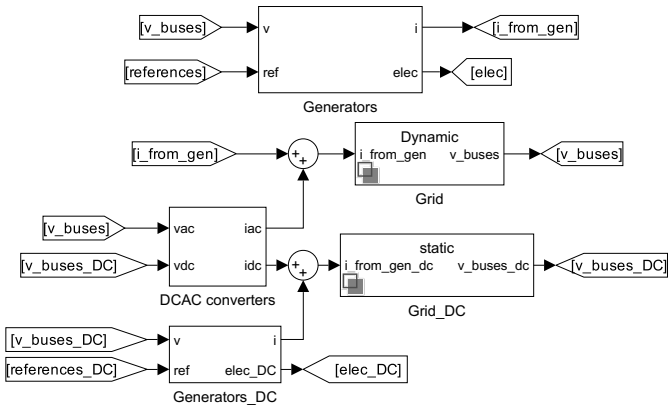

Figure 10: Screenshot of the Simulink workspace for the hybrid system implemented in VFlexP.

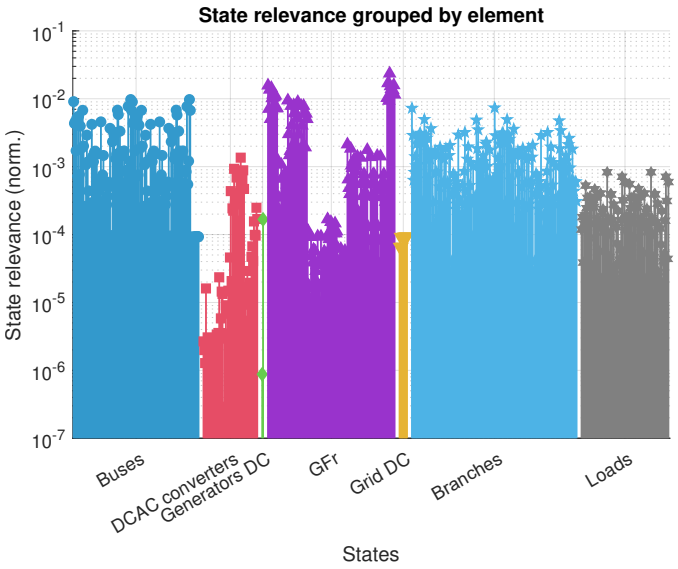

Figure 11: State relevance of the linearised system, grouped by element. The state relevance is normalised to sum one and shown in a logarithmic scale for clarity.

evance". The complete non-linear model of the power system can be used to study the performance of the control loops designed for a grid-following converter. However, this may be computationally expensive or even impractical in some cases. Instead, the use of reduced-order models of the power system based on the information given by the state relevance can be proposed. In this section, simulation results using a full-order linear approximation of the whole system in Fig. 9 at an operating point when bus 101 is perturbed by a grid-following converter will be compared with simulation results using several reduced-order models of the same power system. State relevance has been calculated by injecting a current perturbation at bus 101 and measuring the voltage response of the same bus.

Figure 14 shows the comparison of the response of the frequency measured by the PLL of the grid-following converter to an increment of the active power injected by the grid-following converter placed at bus 101. It includes a

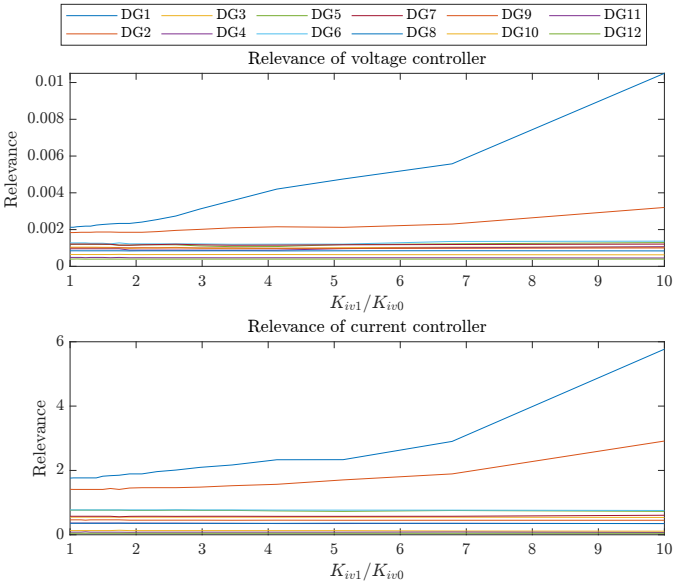

Figure 12: Evolution of the state relevance of the voltage and current controllers for all converters of the system under study when varying the voltage controller of converter DG1. In K_{iv1}/K_{ivO}, K_{iv1} is the varying gain of DG1 and K_{ivO} is its initial value.

comparison between the different linear models described below:

- Full-order approximation to the non-linear system: This is the complete linear model, using the exact block-by-block linearisation of MATLAB/Simulink.
- Reduced-order balanced realisation: A balanced realisation of the system was calculated following the procedure in [36]. Then, the dynamics of the states of the system contributing less to the input-output response were discarded by making their derivatives equal to 0. The states of the system contributing less to the input-output response can be easily identified in this transformation. However, those states are linear combinations of the states of the original system and no longer have a physical meaning.
- Reduced diagonal: The states of the system are transformed with the eigenvectors of the state matrix of the full-order system to have a complex diagonal state matrix with the system eigenvalues on the diagonal. Then, the dynamics of the states of the system contributing less to the input-output response are discarded by making their derivatives equal to 0. The states of the system contributing less to the input-output response are the ones that have large participations from the eigenvalues contributing less to the input-output response. As in the "reduced balance", the states of the transformed system no longer have the same physical meaning as in the original system.
- Truncated original: The state matrix of the full-order linear system was split into relevant and non-

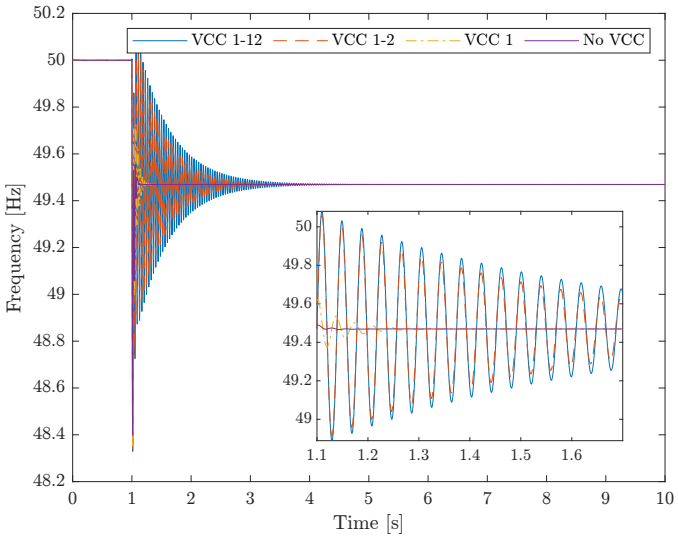

Figure 13: Response of the frequency of DG1 to a load change. Comparison between the complete model and different reduced-order non-linear models.

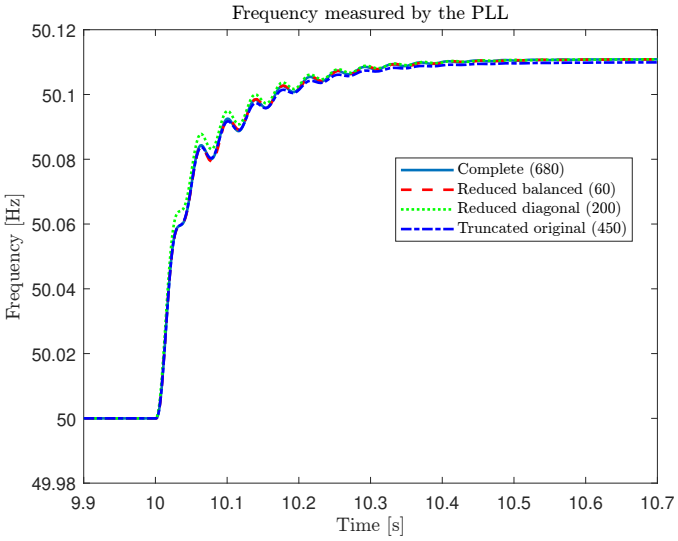

Figure 14: Response of the frequency measured by the PLL of the grid-following converter to an increment of the active power injected by the grid-following converter. Comparison between the complete model and different reduced-order linear models. The number of states of each linear system is shown in brackets.

relevant states, and only the piece corresponding to the relevant states was taken. In this approach, the steady-state value of the response of the full-order system is not matched, but the states of the reduced-order system retain their physical meaning.

5. Conclusion

This paper presented VFlexP, a MATLAB/Simulink-based tool for simulation and analysis of hybrid AC/DC power systems. It includes steady-state analysis, non-linear electromagnetic simulation in a d-q synchronously rotating reference frame, accurate linearisation of the non-linear dynamic model, rich eigenvalue analysis of the linear system, and a tool to assess the relevance of state-variable dynamics in an input-output representation of the power system. This last feature is unique, to the best of the authors' knowledge, and can be used to investigate reduce-order models for further studies. System data can be introduced in a spreadsheet compatible with MATPOWER and the user interface of VFlexP makes it possible an intuitive selection of the complexity with which each system element is to be represented. All elements of the same type with the same level of detail can be included in a single block in Simulink workspace, thanks to the vectorised formulation used, to provide a simple and clear view of even mid-to-large power systems.

The capabilities of VFlexP have been compared with those of a recently published tool, namely, Simplus. The former achieves a more accurate initialisation, which is very useful to avoid unnecessary initial transients when simulating and calculating the operating point for linearisation. In addition, the results of the linearisation process of the former are also more explicable than those of the latter.

Although VFlexP already shows useful features and efficient simulation to address many challenges in modern power systems with a rapidly increasing contribution of electronic power converters in the generation mix, the tool will be extended to address, for example, unbalanced systems as described in [42].

Acknowledgements

This work has been partially financed through the research program S2018/EMT-4366 PROMINT-CAM on Smart Grids of Madrid Government, Spain, with 50% support from the European Social Fund (ESF),

and through Grant TED2021-130610B-C22 funded by MICIU/AEI/10.13039/501100011033 and by European Union NextGenerationEU/PRTR.

The collaboration between Durham University and Comillas has been eased with a special grant to Andrés Tomás-Martín from Comillas Pontifical University for temporary stays of researchers in foreign research centres.

This work is also a collaboration with the project PID2021-125628OB-C21 funded by MICIU/AEI/10.13039/501100011033 and by ERDF/EU, and the Grant PRE2022-101606 funded by MICIU/AEI/10.13039/501100011033 and by ESF+.

Appendix A. Test System Parameters

The parameters for the systems depicted in Figures 3 and 7 are provided in Tables A.6 and A.7, respectively.

Table A.6: Parameters for the system shown in Fig. 3, which can be found in [25].

Synchronous Generator			
H	3.500 s	L_{m_d}	0.04 pu
D	1.00 pu	L_{m_q}	0.04 pu
f	50.0Hz	R_f	0.01 pu
D	1.00 pu	L_f	0.01 pu
R_s	0.01 pu	L_s	0.05 pu
Load			
P_d	0.50 pu	Q_d	0.10 pu

Table A.7: Parameters for the system depicted in Fig. 7, which can be found in [25].

Synchronous Generator			
H	3.500 s	L_{m_d}	0.04 pu
D	1.00 pu	L_{m_q}	0.04 pu
f	50.0 Hz	R_f	0.01 pu
D	1.00 pu	L_f	0.01 pu
R_s	0.01 pu	L_s	0.05 pu
Load			
P_1	0.50 pu	P_2	0.50 pu
P_3	0.50 pu		
Branches			
R_{12}	0.01 pu	X_{12}	0.03 pu
R_{34}	0.01 pu		
Buck Converter			
R	0.01 pu	L	0.00016 pu
K_P	0.6	K_I	565
Interface Converter			
R_f	0.0001 pu	L_f	0.15 pu
K_{PC}	1	K_{IC}	10
$K_{P,PLL}$	1	$K_{I,PLL}$	20
α	0	β	0
γ	0		
$K_{P,DC}$	0.5	$K_{I,DC}$	10

Appendix B. Electronic converter modelling

The control structure and parameters used for grid-forming converters are shown in Figure B.15 and Table B.8, respectively.

All lines were modelled with a Π block, and all loads were modelled as series RL with constant impedance consuming the active and reactive power calculated by the power flow, with the bus voltage also calculated by the power flow solution. The DC/AC interface converters are controlled as grid-following converters, tracking the voltage and angle at their point of connection by means of a phase-locked loop (PLL), with a PI current control loop and a L output filter. The details of the control structure of the converters can be found in [31]. Converter losses were included as in [8] and [41] as a function of the AC output active power:

$$P_{\text{loss},i} = \alpha_i + \beta_i P_i^{AC} + \gamma_i (P_i^{AC})^2 \tag{B.1}$$

Table B.8: Parameters used for the simulation of the large hybrid power system. Control parameters are valid for per-unit variables. The base power is $Sb = 100$ MVA, and the base voltage for every bus can be found in [41].

Grid-forming converters			
m_P	0.0159 pu	n_Q	0.0083 pu
R_f	0.001 pu	L_f	0.01 pu
C_f	1 pu	R_{cf}	1000 pu
R_c	0.001 pu	L_c	0.01 pu
K_{PV}	0.028	K_{IV}	0.28
K_{PC}	34.72	K_{IC}	347.2
F_i	1	LPF_{const}	0.01 s
R_{VI}	0	L_{VI}	0
Interface converters			
$R_{f_{1,4}}$	0.051 pu	$L_{f_{1,4}}$	0.033 pu
$R_{f_{2,3,5,6,7,8}}$	0.0765 pu	$L_{f_{2,3,5,6,7,8}}$	0.05 pu
K_{PC}	1	K_{IC}	10
$K_{P,PLL}$	1	$K_{I,PLL}$	10
α	0.0001	β	0.005
γ	0.05		
$K_{P,DC_{1,4}}$	0.5	$K_{I,DC_{1,4}}$	10

where $P_{loss,i}$ is the active power loss of the converter in per unit, P_i^{AC} is its active power measured on the AC side in per unit, and α_i, β_i, and γ_i are constant values used in all converters:

$$\alpha_i = 0.0001 \quad \beta_i = 0.005 \quad \gamma_i = 0.05 \tag{B.2}$$

Grid-following converters orientate their d-q injected current with respect to the voltage at their AC point of connection and adjust their injected current to meet specific active and reactive power requirements. This alignment is achieved using a phase-locked loop.

The set points for the d- and q-axis currents are calculated using the voltage values on the d and q axes, v_{odi} and v_{oqi}, measured at the connection point, along with the active and reactive power set points P_i^{ref} and Q_i^{ref}:

$$i_{ldi}^* = \frac{v_{odi} P_i^{\text{ref}} + v_{oqi} Q_i^{\text{ref}}}{v_{odi}^2 + v_{oqi}^2} \tag{B.3}$$

$$i_{lqi}^* = \frac{v_{oqi} P_i^{\text{ref}} - v_{odi} Q_i^{\text{ref}}}{v_{odi}^2 + v_{oqi}^2} \tag{B.4}$$

The active and reactive power set points P_i^{ref} and Q_i^{ref} for INV(2,3,5-8), as well as the reactive power set points for INV1 and INV4, were maintained constant with the values derived from the power flow result.

For INV1 and INV4, the active power set points were adjusted to maintain their DC voltage using a PI controller:

$$P_2^{\text{ref}}(s) = (v_{DC,2} - v_{DC,2}^{\text{ref}}) \left(K_{P,DC,2} + \frac{K_{I,DC,2}}{s} \right) \tag{B.5}$$

References

[1] M. O'Malley, T. Bowen, J. Bialek, M. Braun, N. Cutululis, T. Green, A. Hansen, E. Kennedy, J. Kiviluoma, J. Leslie, Y. Li,

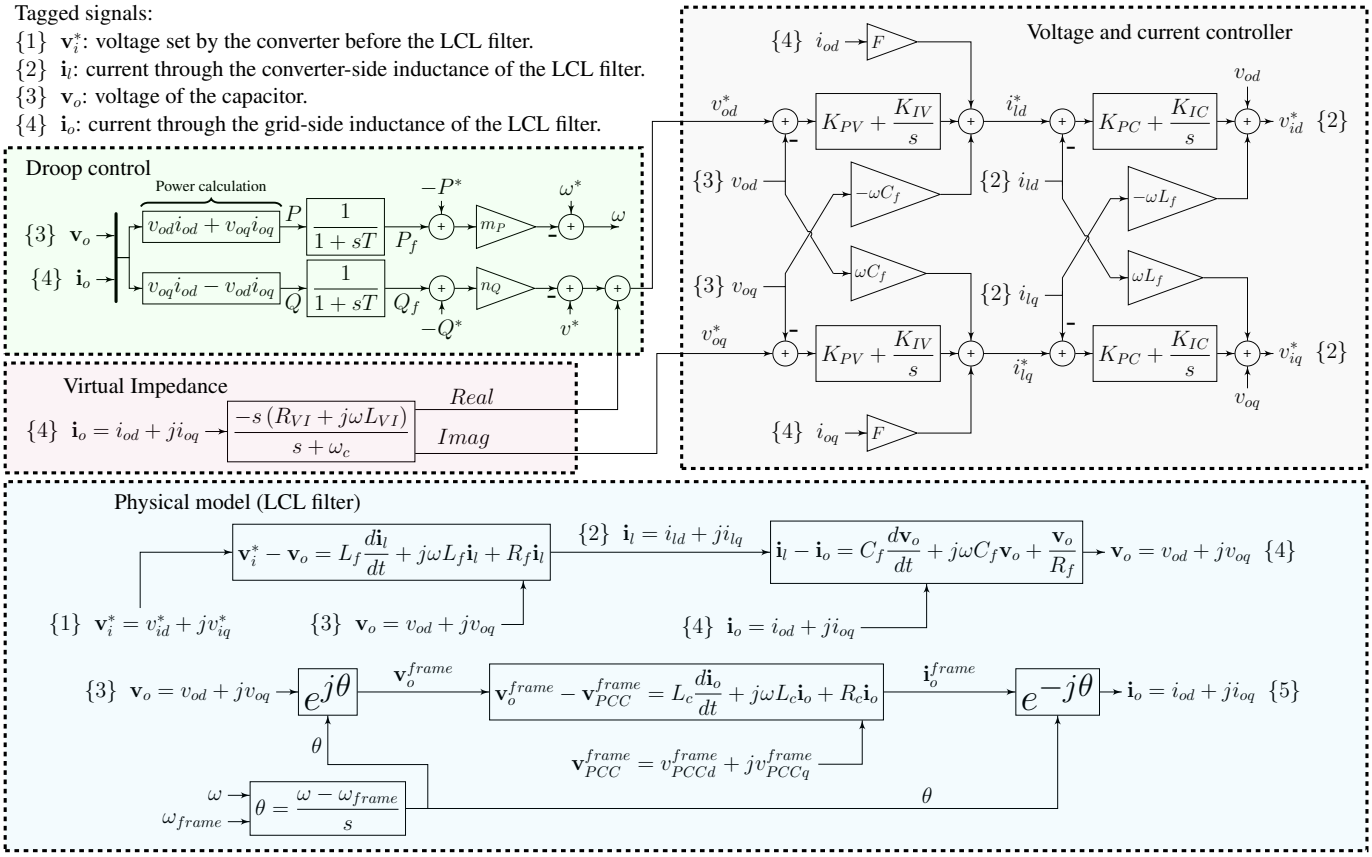

Figure B.15: Model of a grid-forming converter

J. Matevosyan, J. McDowell, N. Miller, P. Pettingill, D. Ramasubramanian, L. Robinson, C. Schaefer, and J. Ward, "Enabling power system transformation globally: A system operator research agenda for bulk power system issues," *IEEE Power and Energy Magazine*, vol. 19, no. 6, pp. 45–55, 2021.

[2] F. Milano, *Power System Modelling and Scripting*. London: Springer-Verlag, 2010.

[3] Chow J.H., Ed., *Time-Scale Modeling of Dynamic Networks with Applications to Power Systems*, ser. Lecture Notes in Control and Information Sciences. New York: Springer-Verlag, 1982, vol. 46.

[4] IEEE-PES, "Simulation methods, models, and analysis techniques to represent the behaviour of bulk power system connected inverter-based resources," IEEE, Technical Report PES-TR113, 2023.

[5] M. Xiong, B. Wang, D. Vaidhynathan, J. Maack, M. J. Reynolds, A. Hoke, K. Sun, and J. Tan, "ParaEMT: An open source, parallelizable, and HPC-compatible EMT simulator for large-scale IBR-rich power grids," *IEEE Transactions on Power Delivery*, vol. 39, no. 2, pp. 911–921, 2024.

[6] P. Kundur, N. J. Balu, and M. G. Lauby, *Power System Stability and Control*, ser. The EPRI Power System Engineering Series. New York: McGraw-Hill, 1994.

[7] R. D. Zimmerman, C. E. Murillo-Sánchez, and R. J. Thomas, "MATPOWER: Steady-State Operations, Planning, and Analysis Tools for Power Systems Research and Education," *IEEE Transactions on Power Systems*, vol. 26, no. 1, pp. 12–19, Feb. 2011.

[8] A. Alvarez-Bustos, B. Kazemtabrizi, M. Shahbazi, and E. Acha-Daza, "Universal branch model for the solution of optimal power flows in hybrid AC/DC grids," *International Journal of Electrical Power & Energy Systems*, vol. 126, p. 106543, Mar. 2021.

[9] J. Beerten and R. Belmans, "MatACDC - an open source software tool for steady-state analysis and operation of hvdc grids," in *11th IET International Conference on AC and DC Power Transmission*, 2015, pp. 1–9.

[10] "PyACDCPF," https://github.com/coek34/PyACDCPF, last Accessed: 26-Jun.-2024.

[11] DIgSILENT, "PowerFactory," Last accessed: 27-Oct-2024. [Online]. Available: https://www.digsilent.de/en/powerfactory.html

[12] Manitoba Hydro International Ltd., "PSCAD," Last accessed: 27-Oct-2024. [Online]. Available: https://www.pscad.com

[13] ETAP-Operation Tecnology, Inc., "ETAP," Last accessed: 27-Oct-2024. [Online]. Available: https://www.etap.com/

[14] Siemens PTI, "PSS/E," Last accessed: 27-Oct-2024. [Online]. Available: https://www.siemens.com/global/en/products/energy/grid-software/planning/pss-software/pss-e.html

[15] D. Serrano-Jiménez, E. Unamuno, A. G. de Muro, D. Aragon, S. Ceballos, and J. Barrena, "Stability tool for electric power systems with a high penetration of electronic power converters," *Electric Power Systems Research*, vol. 210, p. 108115, 2022.

[16] "DSATools," https://www.dsatools.com/overview/, last Accessed: 28-Jun.-2024.

[17] PSI Neplan AG, "NEPLAN," Last accessed: 27-Oct-2024. [Online]. Available: https://neplan.ch/en-products/

[18] D. Shu, X. Xie, V. Dinavahi, C. Zhang, X. Ye, and Q. Jiang, "Dynamic phasor based interface model for emt and transient stability hybrid simulations," *IEEE Transactions on Power Systems*, vol. 33, no. 4, pp. 3930–3939, 2018.

[19] EUROSTAG, "SMART FLOW," Last accessed: 27-Oct-2024. [Online]. Available: https://www.eurostag.be/

[20] H. Cui, F. Li, and K. Tomsovic, "Hybrid symbolic-numeric framework for power system modeling and analysis," *IEEE Transactions on Power Systems*, vol. 36, no. 2, pp. 1373–1384, 2021.

[21] Mirz, M., Dinkelbach, J., and Vogel, S., "DPsim," Last accessed: 28-Oct-2024. [Online]. Available: https://dpsim.fein-aachen.org/docs/

[22] J. D. Lara, R. Henriquez-Auba, M. Bossart, D. S. Callaway, and C. Barrows, "PowerSimulationsDynamics.jl – an open source modeling package for modern power systems with inverter-based resources," 2024, Last accessed: 28-Oct.-2024. [Online]. Available: https://arxiv.org/abs/2308.02921

[23] S. Cole and R. Belmans, "MatDyn, A New Matlab-Based Toolbox for Power System Dynamic Simulation," *IEEE Transactions on Power Systems*, vol. 26, no. 3, pp. 1129–1136, Aug. 2011.

[24] F. Milano, "An open source power system analysis toolbox," *IEEE Transactions on Power Systems*, vol. 20, no. 3, pp. 1199–1206, Aug. 2005.

[25] "Simplus grid tool," https://github.com/Future-Power-Networks/Simplus-Grid-Tool, accessed: 2024-06-26.

[26] Institute for Automation of Complex Power Systems, EONERC, "SSMD," Last accessed: 27-Oct-2024. [Online]. Available: https://www.fein-aachen.org/en/projects/ssmd/

[27] N. Hatziargyriou, J. Milanovic, C. Rahmann, V. Ajjarapu, C. Canizares, I. Erlich, D. Hill, I. Hiskens, I. Kamwa, B. Pal, P. Pourbeik, J. Sanchez-Gasca, A. Stankovic, T. Van Cutsem, V. Vittal, and C. Vournas, "Definition and classification of power system stability – revisited & extended," *IEEE Transactions on Power Systems*, vol. 36, no. 4, pp. 3271–3281, 2021.

[28] J. Tabernero and L. Rouco, "Dynamic Patterns in Small-signal Models of Multipole Synchronous Generators for Wind Power Applications," in *2007 IEEE Lausanne Power Tech*. IEEE, pp. 225–231.

[29] L. Rouco and J. Zamora, "Dynamic patterns and model order reduction in small-signal models of doubly fed induction generators for wind power applications," in *2006 IEEE Power Engineering Society General Meeting*, 2006, pp. 8 pp.–.

[30] R. Griñó, R. Ortega, E. Fridman, J. Zhang, and F. Mazenc, "A behavioural dynamic model for constant power loads in single-phase ac systems," *Automatica*, vol. 131, p. 109744, 2021.

[31] A. Bidram, A. Davoudi, and F. L. Lewis, "A Multiobjective Distributed Control Framework for Islanded AC Microgrids," *IEEE Transactions on Industrial Informatics*, vol. 10, no. 3, pp. 1785–1798, 2014.

[32] S. D'Arco and J. A. Suul, "Virtual synchronous machines — Classification of implementations and analysis of equivalence to droop controllers for microgrids," in *2013 IEEE Grenoble Conference*, 2013, pp. 1–7.

[33] P. W. Sauer and M. A. Pai, *Power System Dynamics and Stability*. Upper Saddle River, N.J: Prentice Hall, 1998.

[34] I. Pérez-Arriaga, G. Verghese, and F. Schweppe, "Selective Modal Analysis with Applications to Electric Power Systems, PART I: Heuristic Introduction," *IEEE Transactions on Power Apparatus and Systems*, vol. PAS-101, no. 9, pp. 3117–3125, Sep. 1982.

[35] A. Tomás-Martín, A. García-Cerrada, L. Sigrist, S. Yagüe, and J. Suárez-Porras, "State relevance and modal analysis in electrical microgrids with high penetration of electronic generation," *International Journal of Electrical Power & Energy Systems*, vol. 147, p. 108876, May 2023.

[36] A. Laub, M. Heath, C. Paige, and R. Ward, "Computation of system balancing transformations and other applications of simultaneous diagonalization algorithms," *IEEE Transactions on Automatic Control*, vol. 32, no. 2, pp. 115–122, Feb. 1987.

[37] J. Van Ness, J. Boyle, and F. Imad, "Sensitivities of large, multiple-loop control systems," *IEEE Transactions on Automatic Control*, vol. 10, no. 3, pp. 308–315, 1965.

[38] F. Pagola, I. Perez-Arriaga, and G. Verghese, "On sensitivities, residues and participations: Applications to oscillatory stability analysis and control," *IEEE Transactions on Power Systems*, vol. 4, no. 1, pp. 278–285, Feb. 1989.

[39] OPAL-RT, "Real-time simulation solutions," Last accessed: 27-Oct-2024. [Online]. Available: https://www.opal-rt.com/

[40] Q. Zheng, F. Gao, Y. Li, Y. Zhu, and Y. Gu, "Equivalence of impedance participation analysis methods for hybrid ac/dc power systems," *IEEE Transactions on Power Systems*, vol. 39, no. 2, pp. 3560–3574, 2024.

[41] R. Chai, B. Zhang, J. Dou, Z. Hao, and T. Zheng, "Unified power flow algorithm based on the NR method for hybrid AC/DC grids incorporating VSCs," *IEEE Transactions on Power Systems*, vol. 31, no. 6, pp. 4310–4318, 2016.

[42] S. J. Yague, A. García-Cerrada, and P. P. Farré, "Comparison between Modal Analysis and Impedance-Based Methods for Analysing Stability of Unbalanced Microgrids with Grid-Forming Electronic Power Converters," *Journal of Modern Power Systems and Clean Energy*, pp. 1–13, 2023.